

QC11, HKUST, July 9, 2011

Probing Emergent Particles and Fields in Quantum Spin Liquids

Yi Zhou (周毅)

Zhejiang University, Hangzhou

Under the collaboration with [Patrick A. Lee](#) (MIT)

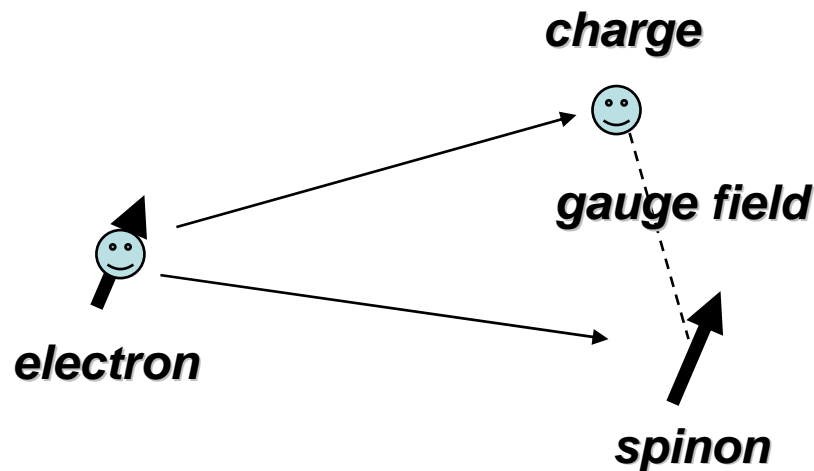
Reference: Phys. Rev. Lett. 106, 056402 (2011)

Quantum spin liquid

- *Quantum spin liquid is an insulator with an odd number of electrons per unit cell which does **not** order magnetically down to zero temperature due to quantum fluctuations.*

Quantum spin liquids as an emergent phenomena

- ***Emergent phenomena***
 - New particles and fields **emerge** at **low-energy scales** but they are totally **absent** in the Hamiltonian that describes the initial system.
 - **Different physics law emerge at different scales.**



$$\hat{c}^+ = \hat{f}^+ \hat{h},$$

$$\hat{f} \rightarrow e^{i\theta} \hat{f},$$

$$\hat{h} \rightarrow e^{i\theta} \hat{f}.$$

**Mathematical form &
U(1) gauge structure**

Emergent particles and fields

- Spinons: $S=1/2$, charge neutral, mobile objects;
 - The spinons *may obey Fermi or Bose statistics* and *there may or may not be an energy gap*;
- Gauge field: *These spinons are generally accompanied by gauge fields, $U(1)$ or Z_2 .*

↑
*constraints to impose single
occupation in a Mott insulator*

nonsense ?

A **dream** of condensed matter theorist

- *A clean example and platform for strongly correlated electrons at $D > 1$*
- *A promising door to the emergent world*

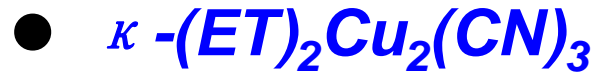


Decades of searching

Realistic material where quantum spin liquid is hosted

Existing spin liquid candidates at $D > 1$

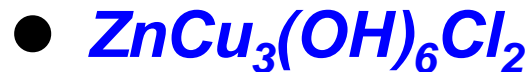
- 2D examples:



$S=1/2$, triangular lattice, organic

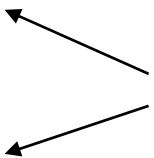


$S=1/2$, triangular lattice, organic



$S=1/2$, kagome lattice

best studied



- 3D spin liquids: Na₄Ir₃O₈

$S=1/2$, hyperkagome lattice, a spinel related oxide

Spin Liquid State in an Organic Mott Insulator with a Triangular Lattice

Y. Shimizu,^{1,2} K. Miyagawa,² K. Kanoda,^{2,3} M. Maesato,¹ and G. Saito¹

¹*Division of Chemistry, Graduate School of Science, Kyoto University, Oiwakekyo, Kitashirakawa, Sakyo-ku, Kyoto, 606-8502, Japan*

²*Department of Applied Physics, University of Tokyo, Hongo, Bunkyo-ku, Tokyo, 113-8656, Japan*

³*CREST, Japan Science and Technology Corporation (JST), Kawaguchi, Saitama, 332-0012, Japan*

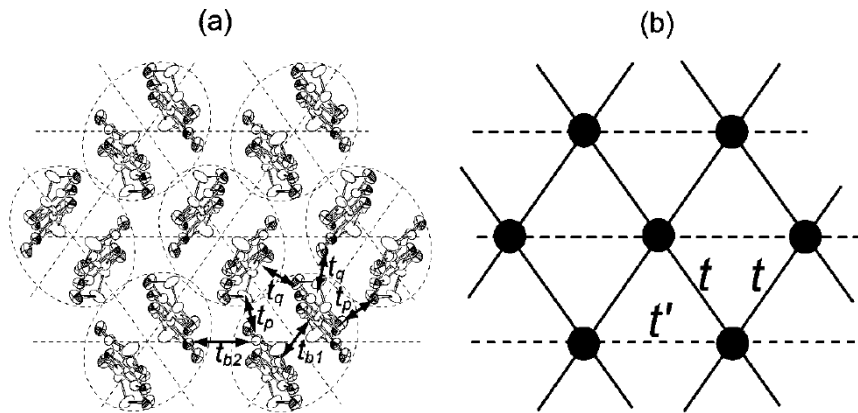


FIG. 1. (a) Crystal structure of an ET layer of κ -(ET)₂Cu₂(CN)₃ viewed along the long axes of ET molecules [4]. The transfer integrals between ET molecules, t_{b1} , t_{b2} , t_p , and t_q , are calculated as 224, 115, 80, and -29 meV, respectively [5]. For the large t_{b1} compared with other transfer integrals, the face-to-face pair of ET molecules connected with t_{b1} can be regarded as a dimer unit consisting of the triangular lattice. (b) Schematic representation of the electronic structure of κ -(ET)₂X, where the dots represent the ET dimer units. They form the anisotropic triangular lattice with $t = (|t_p| + |t_q|)/2$ and $t' = t_{b2}/2$.

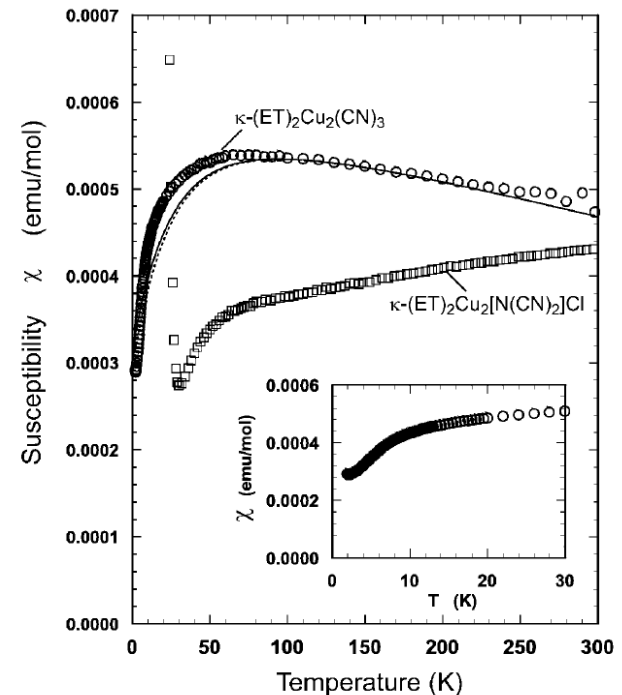


FIG. 2. Temperature dependence of the magnetic susceptibility of the randomly orientated polycrystalline samples of κ -(ET)₂Cu₂(CN)₃ and κ -(ET)₂Cu₂[N(CN)₂]Cl [9]. The core diamagnetic susceptibility is already subtracted. The solid and dotted lines represent the result of the series expansion of the triangular-lattice Heisenberg model using [6/6] and [7/7] Padé approximants, respectively, with $J = 250$ K. The low-temperature data of κ -(ET)₂Cu₂(CN)₃ below 30 K are expanded in the inset.

Quantum spin liquid in the spin-1/2 triangular antiferromagnet $\text{EtMe}_3\text{Sb}[\text{Pd}(\text{dmit})_2]_2$

T. Itou,¹ A. Oyamada,¹ S. Maegawa,¹ M. Tamura,² and R. Kato²

¹Graduate School of Human and Environmental Studies, Kyoto University, Kyoto 606-8501, Japan

²Condensed Molecular Materials Laboratory, RIKEN and JST-CREST, Wako-shi, Saitama 351-0198, Japan

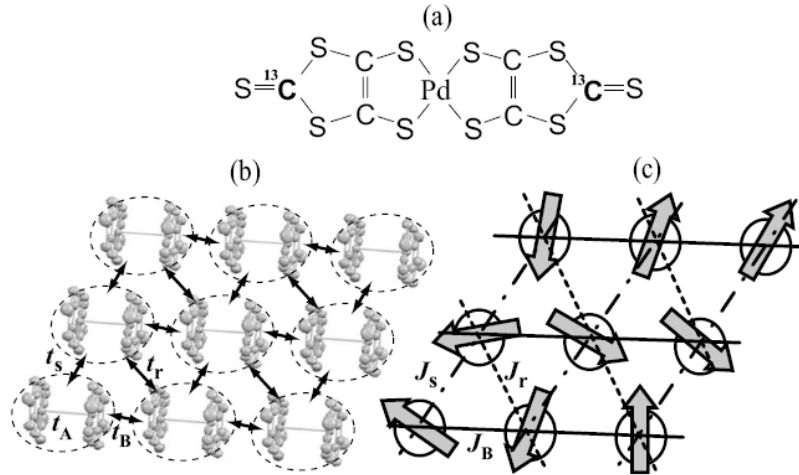


FIG. 1. (a) $\text{Pd}(\text{dmit})_2$ molecule with selective substitution of ^{13}C isotope. The carbon atoms at both ends of the molecule are enriched. (b) Crystal structure of a $\text{Pd}(\text{dmit})_2$ layer viewed along the long axis of the $\text{Pd}(\text{dmit})_2$ molecule. Arrows (t_B , t_S , and t_r) indicate the transfer integral network between the $[\text{Pd}(\text{dmit})_2]_2$ dimers. For $\text{EtMe}_3\text{Sb}[\text{Pd}(\text{dmit})_2]_2$, t_B , t_S , and t_r are calculated using the extended Hückel method as 28.3, 27.7, and 25.8 meV, respectively, while the intradimer transfer integral, t_A , is calculated as 453.5 meV. (c) Schematic of the spin system of $X[\text{Pd}(\text{dmit})_2]_2$, where circles represent $[\text{Pd}(\text{dmit})_2]_2$ dimers on which localized 1/2 spins exist. Three exchange interactions (J_B , J_S , and J_r) are non-equivalent but close to each other, reflecting the values of t_B , t_S , and t_r .

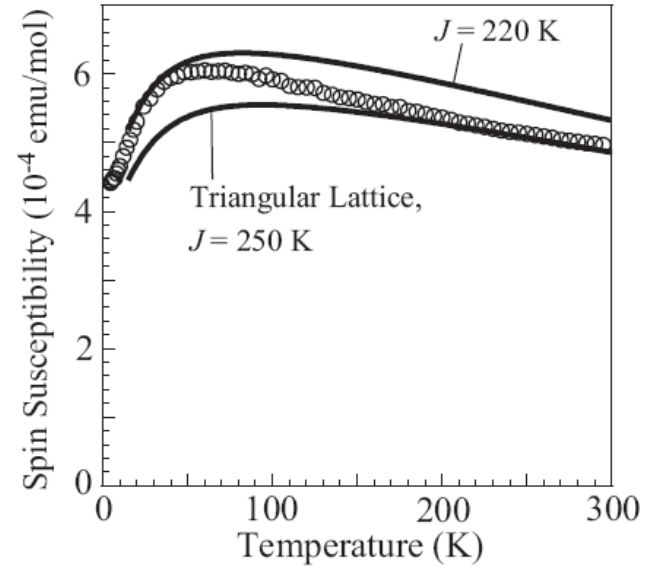
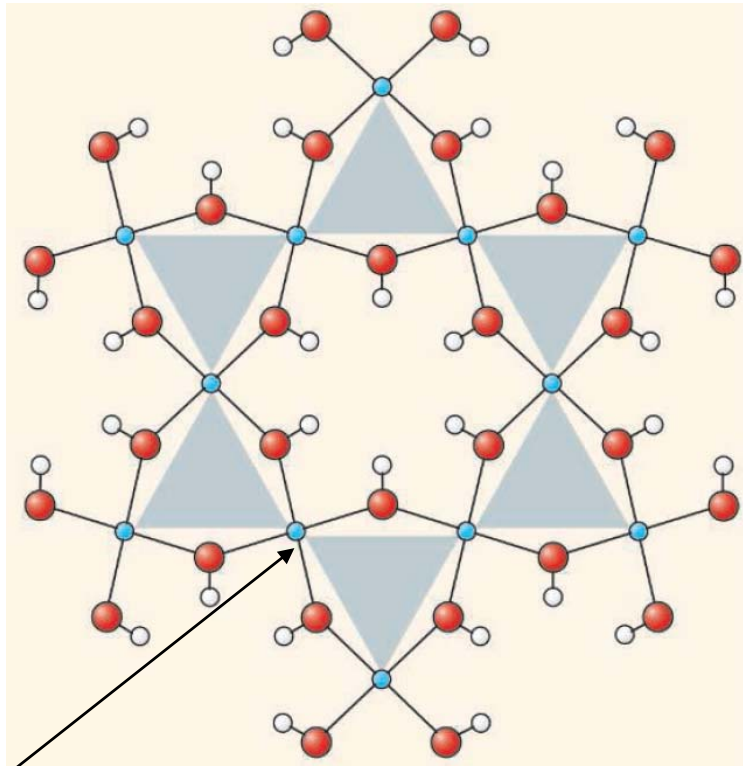


FIG. 2. Temperature dependence of the spin susceptibility of randomly oriented samples of $\text{EtMe}_3\text{Sb}[\text{Pd}(\text{dmit})_2]_2$. Solid curves show the result of the [7/7] Padé approximants for the high-temperature expansion of the regular-triangular antiferromagnetic spin-1/2 system with $J=220$ and 250 K.

Spin Dynamics of the Spin-1/2 Kagome Lattice Antiferromagnet $\text{ZnCu}_3(\text{OH})_6\text{Cl}_2$

J. S. Helton,¹ K. Matan,¹ M. P. Shores,² E. A. Nytko,² B. M. Bartlett,² Y. Yoshida,³ Y. Takano,³ A. Suslov,⁴ Y. Qiu,⁵ J.-H. Chung,⁵ D. G. Nocera,² and Y. S. Lee¹



Cu ion

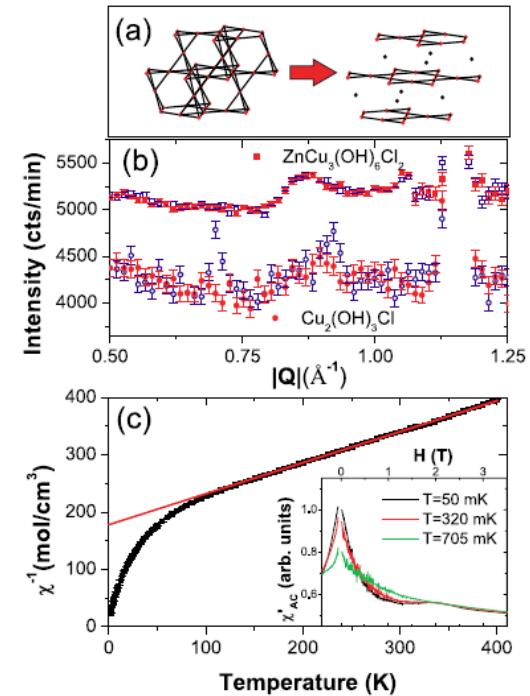


FIG. 1 (color online). (a) The chemical transformation from the pyrochlorelike lattice of $\text{Cu}_2(\text{OH})_3\text{Cl}$ to the kagome layers of $\text{ZnCu}_3(\text{OH})_6\text{Cl}_2$. (b) Magnetic diffraction scans of the two systems at $T = 1.4$ K (open) and 20 K (filled). The $\text{Cu}_2(\text{OH})_3\text{Cl}$ data show magnetic Bragg peaks at $Q \approx 0.70$ and $Q \approx 0.92$, which are absent for the $\text{ZnCu}_3(\text{OH})_6\text{Cl}_2$ data (which have been shifted by 2300 counts/min for clarity). (c) Magnetic susceptibility of $\text{ZnCu}_3(\text{OH})_6\text{Cl}_2$ measured using a SQUID magnetometer plotted as $1/\chi$, where mole refers to a formula unit. The line denotes a Curie-Weiss fit. Inset: ac susceptibility (at 654 Hz) at low temperatures measured at the NIMFL in Tallahassee, FL.

Spin-Liquid State in the $S = 1/2$ Hyperkagome Antiferromagnet $\text{Na}_4\text{Ir}_3\text{O}_8$

Yoshihiko Okamoto,^{1,*} Minoru Nohara,² Hiroko Aruga-Katori,¹ and Hidenori Takagi^{1,2}

¹*RIKEN (The Institute of Physical and Chemical Research), 2-1 Hirosawa, Wako, Saitama 351-0198, Japan*

²*Department of Advanced Materials, University of Tokyo and CREST-JST, 5-1-5 Kashiwanoha, Kashiwa, Chiba 277-8561, Japan*

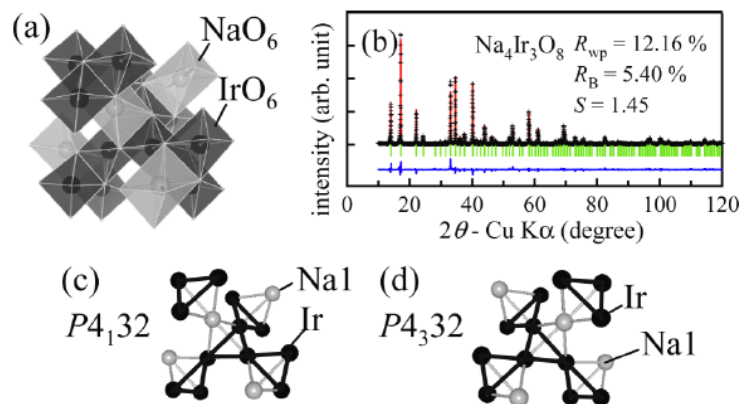


FIG. 1 (color online). (a) Crystal structure of $\text{Na}_4\text{Ir}_3\text{O}_8$ with the space group $P4_132$. Among the three Na sites, only Na1 site is shown for clarity. Black and gray octahedra represent IrO_6 and NaO_6 , respectively. The spheres inside the octahedra represent Ir and Na atoms and oxygens occupy all the corners. (b) The x-ray diffraction pattern of $\text{Na}_4\text{Ir}_3\text{O}_8$ at room temperature. The crosses indicate the raw data and the solid line indicates the spectrum calculated based on the refinement using $P4_132$. (c) and (d) Hyperkagome Ir and Na sublattice derived from the structure of $\text{Na}_4\text{Ir}_3\text{O}_8$ with the space group $P4_132$ (c) and $P4_332$ (d). These two structures with different chirality are indistinguishable by conventional x-ray diffraction, giving the identical result in refinement.

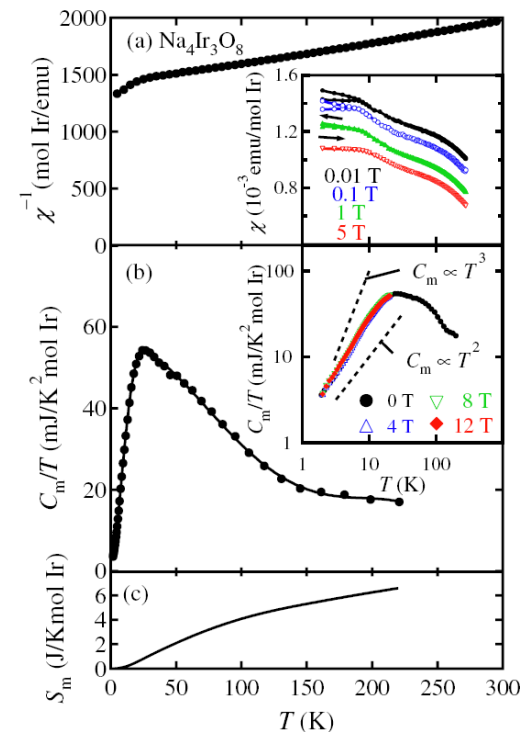


FIG. 2 (color online). Temperature dependence of the inverse magnetic susceptibility χ^{-1} under 1 T (a), magnetic specific heat C_m divided by temperature T (b) and magnetic entropy S_m (c) of polycrystalline $\text{Na}_4\text{Ir}_3\text{O}_8$. To estimate C_m , data for $\text{Na}_4\text{Sn}_3\text{O}_8$ is used as a reference of the lattice contribution. Inset: (a) Temperature dependence of magnetic susceptibility χ of $\text{Na}_4\text{Ir}_3\text{O}_8$ in various fields up to 5 T. For clarity, the curves are shifted by 3, 2, and 1×10^{-4} emu/mol Ir for 0.01, 0.1, and 1 T data, respectively. (b) C_m/T vs T of $\text{Na}_4\text{Ir}_3\text{O}_8$ in various fields up to 12 T. Broken lines indicate C_m proportional to T^2 and T^3 , respectively.

***We shall focus on organic compounds
since they are best studied, but the theory
is generic indeed.***

Experimental Evidences for Mobile fermionic spinons

- **No magnetic order down to 30mK despite $J \approx 250\text{K}$**
- **Linear T dependence of specific heat, Pauli-like spin susceptibility**
S. Yamashita et al., Nature Physics 4, 459 (2008); Nature Comms., 2:275, 1274 (2011).
- **Wilson ratio is close to one**
- **Thermal conductivity**
 - **ET: a large contribution but κ/T is reduced below 0.3K**
M. Yamashita et al., Nature Phys. 5, 44 (2009).
 - **dmit: approach a constant down to the lowest temperature**
M. Yamashita et al., Science 328, 1246 (2010).

Spinons form a Fermi surface and are coupled to $U(1)$ gauge fields

Instability of spinon Fermi surface

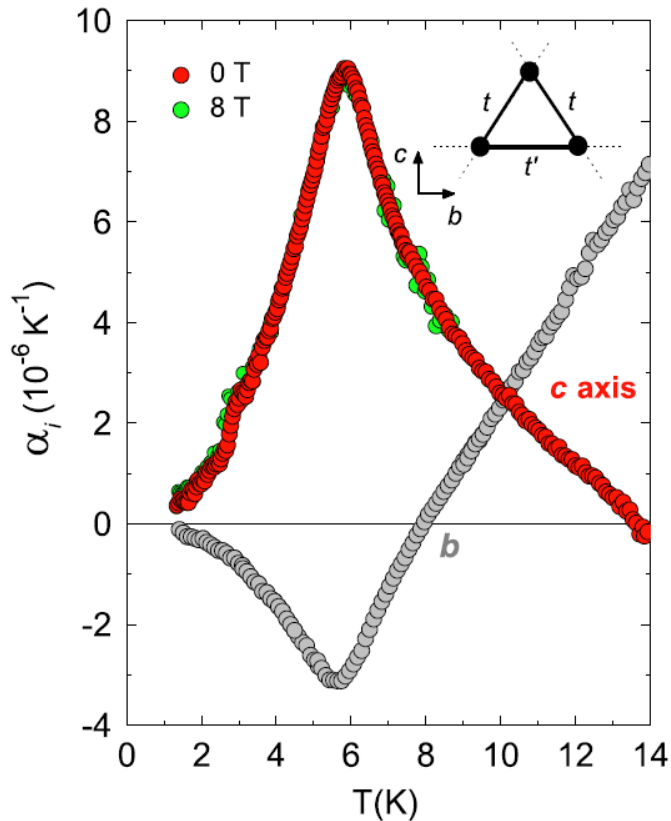


FIG. 2 (color online). In-plane expansivities of κ -(BEDT-TTF)₂Cu₂(CN)₃ on expanded scales with α_c taken in $B = 0$ [dark gray (red) circles] and 8 T [light gray (green) circles]. Inset: 2D triangular-lattice dimer model with hopping amplitudes t' and t .

R. Manna et al, PRL 104, 016403 (2010).

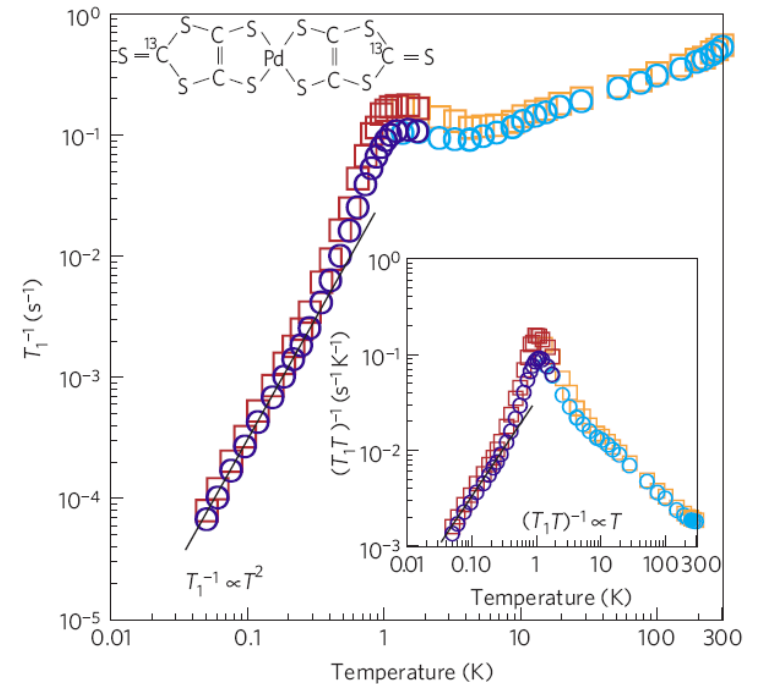


Figure 2 | Temperature dependence of the ¹³C nuclear spin-lattice relaxation rate of EtMe₃Sb[Pd(dmit)₂]₂. The main graph shows the ¹³C nuclear spin-lattice relaxation rate T_1^{-1} of EtMe₃Sb[Pd(dmit)₂]₂, and the inset graph shows $(T_1 T)^{-1}$, where T is temperature. The circles indicate the values determined from the stretched-exponential analysis (see text), and the squares denote the values determined from the initial decay slopes of the relaxation curves. The dark blue circles and dark red squares are obtained from the present measurements below 1.75 K in a dilution refrigerator. For clarity, we did the same analysis for previously reported² higher-temperature data above 1.37 K, and show them here as light blue circles and light red squares. Inset: Pd(dmit)₂ molecule with selective substitution of the ¹³C isotope for the present ¹³C-NMR measurement.

T. Itou et al., Nature Phys. 6, 673 (2010).

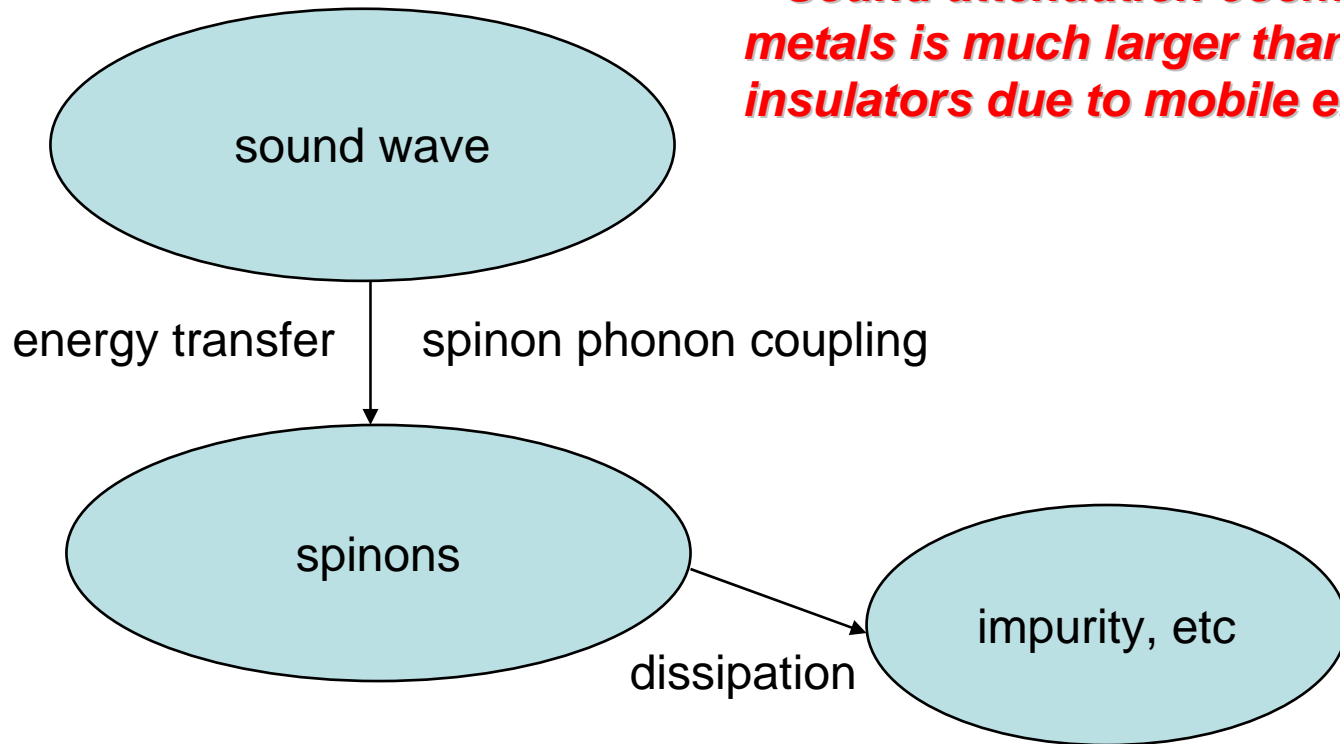
Issues

- We are **not** going to examine the stability or reality of such emergent particles and fields.
- Could we probe spinon and gauge field experimentally?
 - How to measure spinon mass and lifetime?
 - Is there any sharp way to reveal the existence of gauge field experimentally?
- What is the ground state of such a spin liquid?
 - Instability of spinon Fermi surface?
 - Is there a way to **unambiguously** identify the pairing transition of spinons?

Ultrasonic attenuation is a promising way to address these issues.

Process of sound attenuation due to spinons

Sound attenuation coefficient in metals is much larger than that in insulators due to mobile electrons!



a method to measure spinon mass and lifetime

Spinon phonon coupling

Assumption: spinon mean field band, quadratic dispersion

$$H_0 = E_0(\mathbf{p}) + V_{\text{imp}}(\mathbf{r}')$$

$$H_{\text{s-ph}} = \sum_{\mathbf{k}, \mathbf{q}, \lambda, \sigma} M_{\mathbf{k}\lambda}(\mathbf{q}) f_{\mathbf{k}+\mathbf{q}\sigma}^\dagger f_{\mathbf{k}\sigma} (a_{\mathbf{q}\lambda} + a_{-\mathbf{q}\lambda}^\dagger)$$

$$M_{\mathbf{k}\lambda}(\mathbf{q}) = (\mathbf{k} \cdot \hat{\varepsilon}_{\mathbf{q}\lambda}) [\mathbf{q} \cdot \mathbf{v}(\mathbf{k})] (2\rho_{\text{ion}}\omega_{\mathbf{q}\lambda})^{-1/2}$$

It turns out that in the long wavelength limit, the coupling matrix elements are exactly the same as electron !

Microscopic model

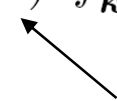
Phonon Hamiltonian: $H_{\text{ph}} = \sum_{\mathbf{q}, \lambda, \sigma} \omega_{\mathbf{q}\lambda} a_{\mathbf{q}\lambda}^\dagger a_{\mathbf{q}\lambda}$

Spinon phonon interaction:

$$H_{\text{s-ph}} = \sum_{\mathbf{k}, \mathbf{q}, \lambda, \sigma} M_{\mathbf{k}\lambda}(\mathbf{q}) f_{\mathbf{k}+\mathbf{q}\sigma}^\dagger f_{\mathbf{k}\sigma} (a_{\mathbf{q}\lambda} + a_{-\mathbf{q}\lambda}^\dagger)$$

Spinon kinetic energy:

$$H_{0s} = \sum_{\mathbf{k}, \sigma} \frac{1}{2m} (\mathbf{k} + \mathbf{a})^2 f_{\mathbf{k}\sigma}^\dagger f_{\mathbf{k}\sigma}$$

 *gauge field, non double occupancy*

Impurity scattering:

$$H_{\text{imp}} = \sum_{i\sigma} v_{\text{imp}}(\mathbf{r}_i) f_\sigma^\dagger(\mathbf{r}_i) f_\sigma(\mathbf{r}_i)$$

elastic scattering, mean free path $l = v_F \tau$

Hydrodynamic limit: $ql \ll 1$

The fermions are treated as a viscous medium

*W. P. Mason, Phy. Rev. 97, 557 (1955);
R. W. Morse, Phy. Rev. 97, 1716 (1955).*

linearized Navier-Stokes equation:

$$\rho \frac{\partial \mathbf{u}}{\partial t} = -\nabla p + \left(\frac{4}{3}\eta + \chi \right) \nabla (\nabla \cdot \mathbf{u}) - \eta \nabla \times \nabla \times \mathbf{u}$$

instantaneous density: $\rho = \rho_0 (1 + s)$

equation of continuity: $\nabla \cdot \mathbf{u} = -\frac{\partial s}{\partial t}$

acoustic pressure:

$$p = \left(\frac{\partial p}{\partial \rho} \right)_{\rho_0} \rho_0 s = \rho_0 v_s^2 s$$

lossy wave equation:

$$\left(1 + \tau_s \frac{\partial}{\partial t} \right) \nabla^2 p = \frac{1}{v_s^2} \frac{\partial^2 p}{\partial t^2}$$

sound wave relaxation time:

$$\tau_s^L = \frac{1}{\rho_{\text{ion}} v_s^2} \left(\frac{4}{3}\eta + \chi \right), \tau_s^T = \frac{1}{\rho_{\text{ion}} v_s^2} \eta$$

monofrequency motion → Helmholtz equation:

$$\nabla^2 p + k^2 p = 0 \qquad k = \frac{\omega}{v_s} \frac{1}{(1+i\omega\tau_s)^{1/2}}$$

attenuation coefficient: $\alpha = -\text{Im}k$

$$\alpha = \frac{1}{\sqrt{2}} \frac{\omega}{v_s} \left[\frac{\sqrt{1 + (\omega\tau_s)^2} - 1}{1 + (\omega\tau_s)^2} \right]^{1/2}$$

In the limit $\omega\tau_s \ll 1$:

$$\alpha = \frac{\omega^2 \tau_s}{2v_s}$$

Fermion viscosity:

$$\eta = \frac{1}{15} N(0) m^2 v_F^4 \tau \qquad \chi \ll \eta$$

Go beyond hydrodynamic limit

- **Pippard's theory for $ql \geq 1$, Boltzmann equation:**

- *The electrons develop local charge and current fluctuation for the longitudinal and transverse phonons which contribute significantly to the sound attenuation;*

A. B. Pippard, Phil. Mag. 41, 1104 (1955); Proc. R. Soc. London, A257, No. 1289, 65 (1960).

- **Tsuneto's theory for superconductor:**

- *A combination of diagrammatic and Boltzmann approach;*
- *Current fluctuations for transverse phonons are ignored;*

T. Tsuneto, Phys. Rev. 121, 402 (1961).

- **Our method:**

- *Diagrammatic approach*

Sound attenuation in a normal metal

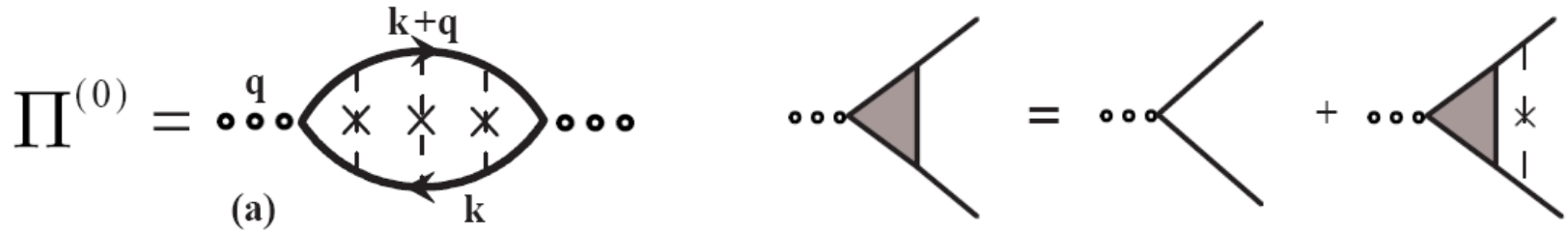
Phonon self energy: $\Pi(q, \omega)$

Impurity averaged fermion Green's function:

$$G_{\text{ret(adv)}}(k, \omega) = \frac{1}{\omega - \xi_k \pm i/2\tau}$$

$$\xi_k = \frac{k^2}{2m} - \mu$$

Longitudinal sound wave



Longitudinal sound attenuation in 3D:

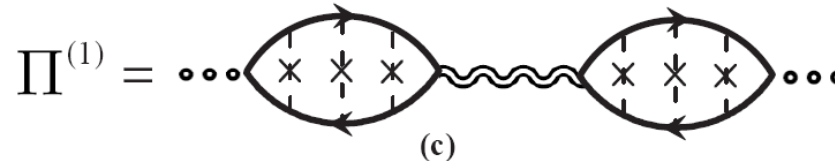
$$\begin{aligned}\alpha &= \frac{\omega N(0) k_F^3}{m \rho_{ion} v_s^2} \frac{1}{3ql} \left[\frac{q^2 l^2 \tan^{-1}(ql)}{ql - \tan^{-1}(ql)} - \frac{1}{3} \right] \\ &= \frac{nm}{\rho_{ion} v_s \tau} \left[\frac{q^2 l^2 \tan^{-1}(ql)}{ql - \tan^{-1}(ql)} - \frac{1}{3} \right],\end{aligned}$$

Longitudinal sound attenuation in 2D:

$$\begin{aligned}\alpha &= -\frac{\omega N(0) k_F^3}{m \rho_{ion} v_s^2} \text{Re} \left\{ t_4(a) - t_2(a) + \frac{1}{4} t_0(a) - \frac{[t_2(a) - \frac{1}{2} t_0(a)]^2}{a + t_0(a)} \right\} \\ &= \frac{nm}{\rho_{ion} v_s \tau} \left[\frac{q^2 l^2}{1 - \sqrt{1 + q^2 l^2}} - \frac{1}{2} \right].\end{aligned}$$

Transverse sound wave

$\Pi^{(1)}$ does not vanish



$\Pi^{(1)}$ takes the remarkably simple form:

$$\Pi_{\text{ret}}^{(1)} = i \frac{1-g}{g} \text{Im} \Pi_{\text{ret}}^{(0)} + O(v_s/v_F)$$

$$\sigma_{\perp}(q, \omega) = g\sigma_0 \quad g = \frac{3}{2a} \text{Re}[s_2(a) - s_0(a)] \quad s_n(a) = \frac{1}{2i} \int_{-1}^1 du \frac{u^n}{u + i/a}$$

where $a = ql/(1 + i\omega\tau) \quad \omega\tau \ll 1 \rightarrow \text{set } a = ql$

Transverse sound relaxation at 3D:

$$\alpha = -\frac{2}{v_s} \text{Im}(\Pi_{\text{ret}}^{(0)} + \Pi_{\text{ret}}^{(1)}) = \frac{nm}{\rho_{\text{ion}} v_s \tau} \frac{1-g}{g}$$

Clean limit $ql \gg 1$: $g \rightarrow \frac{3\pi}{4} (ql)^{-1}$ **$\Pi^{(1)}$ dominates !**

Dirty limit $ql \ll 1$: $g \rightarrow 1 - \frac{2}{15} (ql)^2$

Onset of superconductivity

$\Pi^{(0)}$ decreases below T_c due to the opening of the energy gap

$$\mathcal{G}(\mathbf{k}, i\omega_n) = \frac{i\tilde{\omega}_n + \xi_{\mathbf{k}}}{(i\tilde{\omega}_n)^2 - \xi_{\mathbf{k}}^2 - [\tilde{\Delta}_{\mathbf{k}}(\omega_n)]^2},$$

$$\mathcal{F}(\mathbf{k}, i\omega_n) = -\frac{\tilde{\Delta}_{\mathbf{k}}(\omega_n)}{(i\tilde{\omega}_n)^2 - \xi_{\mathbf{k}}^2 - [\tilde{\Delta}_{\mathbf{k}}(\omega_n)]^2},$$

$$\tilde{\omega}_n = \omega_n \left(1 + \frac{1}{2\tau\sqrt{\omega_n^2 + \Delta_{\mathbf{k}}^2}}\right),$$

$$\tilde{\Delta}_{\mathbf{k}}(\omega_n) = \Delta_{\mathbf{k}} \left(1 + \frac{1}{2\tau\sqrt{\omega_n^2 + \Delta_{\mathbf{k}}^2}}\right),$$

- The fermion lifetime τ should be finite to relax the sound wave.
- $v_s \ll v_F$, despite $q/\ell \geq 1$, the physically relevant situation is reached by $\omega \tau \ll 1$.
- We can not take $\tau \rightarrow \infty$ at first even in the clean limit, because finite τ is still seen for $\omega \tau \ll 1$.
- We shall discuss the limit $\omega \tau \ll 1 \ll \Delta \tau$.


$$\begin{aligned} \text{Im}\Pi_{\text{ret}}^{(0)} &= 2\omega\pi N(0) \text{Re} \int_{-1}^1 d\nu \int_{|\Delta_{\mathbf{k}}|}^{\infty} \frac{d\epsilon}{2\pi} \frac{[M_{\mathbf{k}\lambda}(\mathbf{q})]^2 \left[1 + \frac{\epsilon(\epsilon+\omega) - \Delta_{\mathbf{k}}\Delta_{\mathbf{k}+\mathbf{q}}}{\sqrt{\epsilon^2 - \Delta_{\mathbf{k}+\mathbf{q}}^2} \sqrt{(\epsilon+\omega)^2 - \Delta_{\mathbf{k}}^2}}\right]}{\sqrt{(\epsilon+\omega)^2 - \Delta_{\mathbf{k}}^2} - \sqrt{\epsilon^2 - \Delta_{\mathbf{k}+\mathbf{q}}^2} + i/\tau + qv_F\nu} \left[-\frac{\partial n_F(\epsilon)}{\partial \epsilon}\right] \\ &\simeq 2\omega\pi N(0) \text{Re} \int_{-1}^1 d\nu \int_{|\Delta_{\mathbf{k}}|}^{\infty} \frac{d\epsilon}{2\pi} \left[-\frac{\partial n_F(\epsilon)}{\partial \epsilon}\right] \frac{[M_{\mathbf{k}\lambda}(\mathbf{q})]^2 \left[1 + \frac{\epsilon^2 - \Delta_{\mathbf{k}}\Delta_{\mathbf{k}+\mathbf{q}}}{\sqrt{\epsilon^2 - \Delta_{\mathbf{k}+\mathbf{q}}^2} \sqrt{\epsilon^2 - \Delta_{\mathbf{k}}^2}}\right]}{\sqrt{\epsilon^2 - \Delta_{\mathbf{k}}^2} - \sqrt{\epsilon^2 - \Delta_{\mathbf{k}+\mathbf{q}}^2} + i/\tau + qv_F\nu}. \end{aligned}$$

For a s-wave pairing state,

$$\frac{\alpha^{(0)}}{\alpha_N^{(0)}} = 2n_F(\Delta)$$

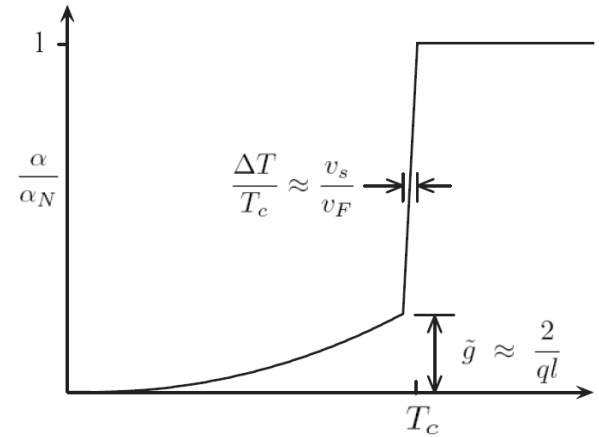
Onset of superconductivity

$\Pi^{(1)}$ drop to zero **rapidly** below T_c

$\Pi^{(1)} =$ 

$$D_{\text{ret}}^{\text{EM}} = \frac{1}{i\omega\sigma_{\perp}(q, \omega) + \omega^2 - c^2q^2}$$

$$\Pi_{\text{ret}}^{(1)} = i \frac{1-g}{g} \text{Im} \Pi_{\text{ret}}^{(0)} + O(v_s/v_F)$$



The fractional size of the drop: $(1 - g)$

 $(\sim \frac{2}{15}(ql)^2)$ for $ql \ll 1$ $(1 - \frac{3\pi}{4ql})$ in the clean limit of $ql \gg 1$

FIG. 2: Schematic plot of the attenuation of transverse sound (for $ql \gtrsim 1$) in a spin liquid normalized to α_N , the value in the Fermi liquid state. The “rapid fall” over a narrow temperature range ΔT at the transition to the spinon paired state is due to the Meissner effect of the gauge field.

Attenuation of transverse sound by spinons

U(1) spin liquid in 2D:

$$D_{\text{ret}}^T = \frac{1}{i\omega\tilde{\sigma}_{\perp}(q, \omega) - \chi q^2}$$

$$\tilde{\sigma}_{\perp} = \tilde{g}\tilde{\sigma}_0, \quad \tilde{\sigma}_0 = n\tau/m \qquad \chi = 1/(24\pi m) \quad \textit{Landau diamagnetism}$$

$$\tilde{g} = \frac{2}{a}[t_2(a) - t_0(a)], \quad t_n(a) = \frac{1}{2i} \int_0^{2\pi} d\theta \frac{\cos^n \theta}{\cos \theta + i/a}.$$

Clean limit:

$$\tilde{g} = \frac{2}{ql} \text{ for } ql \gg 1$$

Dirty limit:

$$\tilde{g} = 1 - \frac{(ql)^2}{4} \text{ for } ql \ll 1$$

When $\chi q^2 \ll \omega\tilde{\sigma}_{\perp}$,

$$\alpha = \frac{nm}{\rho_{\text{ion}} v_s \tau} \frac{1 - \tilde{g}}{\tilde{g}}$$

Measure spinon mass and lifetime

$$\alpha = \frac{nm}{\rho_{\text{ion}} v_s \tau} \frac{1 - \tilde{g}}{\tilde{g}}$$

q -dependence

Rapid drop below T_c : reveal the existence of $U(1)$ gauge field

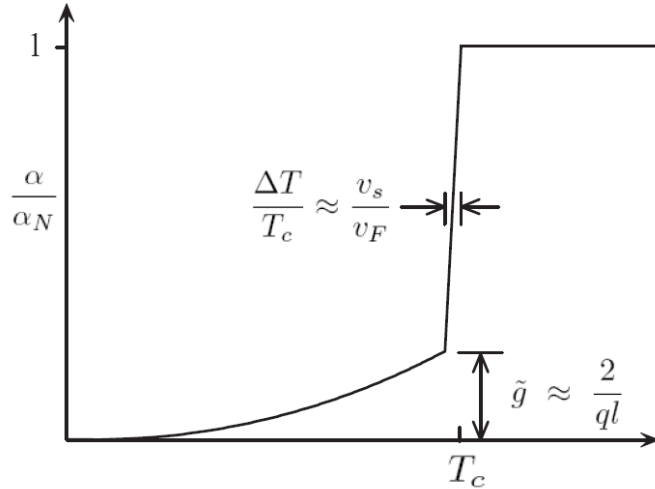


FIG. 2: Schematic plot of the attenuation of transverse sound (for $ql \gtrsim 1$) in a spin liquid normalized to α_N , the value in the Fermi liquid state. The “rapid fall” over a narrow temperature range ΔT at the transition to the spinon paired state is due to the Meissner effect of the gauge field.

$$i\omega\tilde{\sigma}_{\perp} \rightarrow i\omega\tilde{\sigma}_{\perp} - n_s(T)/m$$

$$\frac{\text{Im}\Pi_s^{(1)}}{\text{Im}\Pi_N^{(1)}} = \frac{1}{1 + (n_s(T)/m\omega\tilde{\sigma}_0\tilde{g})^2}$$

$$ql \gg 1, \Pi^{(1)} \text{ dominates}$$

$$\Delta T : \frac{\text{Im}\Pi_s^{(1)}}{\text{Im}\Pi_N^{(1)}} = \frac{1}{2}$$

$$n_s(T) = 2n \frac{\Delta T}{T_c}$$

$$\frac{\Delta T}{T_c} \approx \frac{v_s}{v_F}$$

Summary

- **Spinon phonon coupling**

- We show that despite being charge neutral, the spinons couple to phonons in exactly the same way that electrons do in the long wavelength limit.

- **Use q -dependence of sound attenuation to measure the spinon mass and lifetime**

- **Transverse ultrasonic attenuation is a direct probe of the onset of pairing**

- Meissner effect of the gauge field causes a “rapid fall” of the attenuation coefficient at T_c in addition to the reduction due to the opening of the energy gap.

- **Reveal the existence of the $U(1)$ gauge field**

Thank you !